



An energy-dissipation-based power-law formulation for estimating hemolysis

Peng Wu¹ · Sascha Groß-Hardt² · Fiete Boehning³ · Po-Lin Hsu¹

Received: 18 November 2018 / Accepted: 9 October 2019 / Published online: 14 October 2019
© Springer-Verlag GmbH Germany, part of Springer Nature 2019

Abstract

Hemolysis is a major concern in blood-circulating devices, which arises due to non-physiological stresses on red blood cells from ambient flow environment or moving mechanical structures. Computational fluid dynamics (CFD) and empirical hemolysis prediction models have been increasingly used for the design and optimization of blood-circulating devices. The commonly used power-law models for hemolysis prediction often use Reynolds stress to represent effective stress, tend to over-predict hemolysis and fail to capture trends of flow-related hemolysis. This study proposed a new power-law formulation for the numerical hemolysis prediction. The new formulation related hemolysis to the energy dissipation rate, which could be readily obtained from CFD simulations. The model constants were regressed from existing hemolysis data. The new formulation was tested for three benchmark cases and compared to conventional power-law models. The results showed that the new formulation improved prediction of hemolysis for a broad range of flow regimes. The deviations of the predicted hemolysis from experimental results were within one order, and better correlated with experimental results. This study confirmed that Reynolds stress is the main cause of over-prediction of hemolysis for conventional power-law models. Proportionally, the blood damage predicted with Reynolds stresses is more than one order higher than viscous stress, in terms of energy dissipation.

Keywords Hemolysis · Blood damage · Energy dissipation · Reynolds stress · Blood pump · CFD

1 Introduction

In many blood-circulating devices, such as prosthetic heart valves, ventricular assist devices (VADs) and hemodialysis machines, non-physiological stresses can be up to two orders of magnitude than physiological stresses (Fraser et al. 2011; Garon and Farinas 2004). This increases the risk of blood damage, such as the release of hemoglobin (Hb) into plasma, which is called hemolysis. Computational fluid dynamics (CFD) has become increasingly important for the design and optimization of blood-circulating devices, offering the

possibility to predict hemolysis in a purely numerical manner (Fraser et al. 2011; Garon and Farinas 2004; Park et al. 2005; Rose et al. 2001; Wu et al. 2018a).

Hemolysis estimation models can be primarily divided into theoretical and empirical approaches. Strain-based model and power-law model are two primary examples of these two approaches. Strain-based models (Chen and Sharp 2011; Ezzeldin et al. 2015; Faghih and Sharp 2018; Sohrabi and Liu 2017; Vitale et al. 2014) account for the development of cell membrane tension due to fluid stress, strain of the cell membrane to the point of failure and formation of pores, and transport of hemoglobin through the pores in the membrane, a bottom-up approach. In contrast, power-law models were derived from the empirical observation and regression of in vitro hemolysis data obtained from experiments, a top-down approach. Typical hemolysis estimation models relate hemolysis to effective stress τ and exposure time t through a power-law relationship (Giersiepen et al.

✉ Peng Wu
pwu@suda.edu.cn

¹ Artificial Organ Technology Laboratory, Bio-manufacturing Research Centre, School of Mechanical and Electric Engineering, Soochow University, Suzhou, Jiangsu, China

² Department of Cardiovascular Engineering, Institute of Applied Medical Engineering, Helmholtz Institute, RWTH Aachen University, Aachen, Germany

³ enmodes GmbH, Aachen, Germany

1990; Heuser and Opitz 1980; Wu et al. 2018a; Zhang et al. 2011)

$$\text{HI}(\%) = \frac{\text{hb}}{\text{Hb}} \times 100 = c \tau_{\text{eff}}^{\alpha} t^{\beta}, \quad (1)$$

where HI(%) is the hemolysis index in percentage, τ_{eff} is the effective stress and a scalar quantity, Hb is the total hemoglobin concentration, hb represents the increase in plasma free hemoglobin; c , α and β are empirical constants determined by regression of hemolysis data. Power-law models have been the most popular estimation models to date, probably because of their ease of implementation and apparent broad applicability.

The flow regimes in blood-shearing devices for experimental determination of hemolysis are primarily laminar flows. However, the blood flow in blood-circulating devices occurs in both the laminar and turbulent regimes. It is an extrapolation to apply hemolysis models which were derived from laminar flows to turbulent flows. Jones argued that the hemolysis in turbulent flows is due to instantaneous viscous stress; similar to the fact that hemolysis is mainly due to viscous shear stress in laminar flows (Jones 1995). The strain-based hemolysis models also rely on the flow properties such as instantaneous strain rates at cellular level. Accurate prediction of these quantities at cellular level can only be achieved by direct numerical simulation (DNS). For most practical engineering problems, the computational cost of DNS is prohibitive.

In contrast, as a comprise, turbulence modeling techniques such as large eddy simulation (LES) (Wu et al. 2018b; Wu and Meyers 2013, 2011) and Reynolds-averaged Navier–Stokes (RANS) (Cao and Meyers 2012; Cao et al. 2017) were introduced to reduce computational cost, allowing for less stringent requirement on time and grid resolution. RANS is the most frequently used turbulence modeling technique in blood-circulating devices (Fraser et al. 2011). In RANS method, Reynolds stress is used to account for turbulence effects. In power-law models, effective stress τ_{eff} is often represented using viscous stress τ_{vis} together with Reynolds stress τ_{turb} , to predict hemolysis in hemodynamic flow fields (Arvand et al. 2005; Grigioni et al. 2005; Segalova et al. 2012; Wu et al. 2009):

$$\tau_{\text{eff}} = \tau_{\text{vis}} + \tau_{\text{turb}} = (\mu_t + \mu)S, \quad (2)$$

where μ is viscosity; μ_t is turbulent viscosity, either specified or solved, subject to a specific RANS model; S is the magnitude of strain rate.

However, it is not mathematically validated whether Reynolds stress and mean stress are the true representation for instantaneous viscous stress. Hund et al. (2010) showed that effective stress represented using Reynolds stress results in a systematic error. It has been shown that the Reynolds stress is an inaccurate indicator of turbulent effects on

hemolysis (Ge et al. 2008; Jones 1995; Quinlan and Dooley 2007), and tends to over-predict the level of hemolysis. It is not sensitive to the microscale temporal and spatial scales of the blood cells suspended in turbulent flow (Quinlan and Dooley 2007).

One of most prominent features of turbulent flows is energy cascade, which refers to the transfer of energy from large scales of energy-containing motions to small eddies where viscous dissipation converts kinetic energy into heat by friction. In blood flows, the RBCs are subject to the energy cascade and dissipation processes. One of the primary goals when designing turbulence models is to ensure the correct dissipation rate (Pope 2000). Therefore, from a modeling point of view, it is more reasonable to relate hemolysis to dissipation than Reynolds stress, for hemolysis estimations in turbulent flows.

Some researchers related viscous dissipation to blood damage (Ge et al. 2008; Hund et al. 2010; Morshed et al. 2014; Quinlan 2014). Wu et al. (2019) reformulated existing power-law models by representing effective stress in terms of energy dissipation while keeping the constants unchanged. Their results showed that the representation of effective stress in terms of energy dissipation improved the over-prediction of hemolysis for a wide range of flow conditions. However, the trends of flow-related hemolysis remained unchanged, and differed notably from the measured hemolysis. Based on previous hemolysis data from a capillary tube, Wu et al. (2019) found that the relationship between overall energy dissipation and hemolysis is represented by a single monotonic curve, regardless of laminar or turbulent flow regimes. Moreover, hemolysis is proportional to the overall energy dissipation to the power of 2.27; in contrast, this value is around 1 for mainstream power-law models.

This work proposes a new power-law formulation for estimating hemolysis, which relates hemolysis to energy dissipation. The set of empirical constants were regressed from existing experimental hemolysis data. The new formulation was tested over three benchmark cases with a wide range of flow conditions. The new model improved the prediction of hemolysis in terms of both absolute values and trends.

2 Methods

First, hemolysis rate \bar{h} is introduced and given by

$$\bar{h} = \frac{\text{HI}(\%)}{t}, \quad (3)$$

which represents the degree of hemolysis per unit time. Energy dissipation converts mechanical energy into heat by friction; energy dissipation rate ε is normally used to

describe the power loss per unit volume and unit time. Assuming a power-law relationship between \bar{h} and ϵ :

$$\bar{h} = C\epsilon^{\alpha'} \tag{4}$$

where C and α' are to be determined from regression of hemolysis data. The hemolysis data should cover a broad range of loading conditions, and the flow field in the shearing device should be as uniform as possible.

The hemolysis data of Boehning et al. (2014) were chosen for regression. Figure 1a shows the schematic of their shearing device (referred to as Aachen shearing device hereafter). Wu et al. (2018a) showed the entrance effects are limited to less than 1% of the axial length of the gap. Secondary damage effects due to sealing have been a major concern for blood-shearing devices (Giersiepen et al. 1990, Heuser and Opitz 1980). A sealing fluid (NaCl solution) was used for Aachen shearing device to prevent the sheared blood from contact with air and the bearings, and minimize secondary damage effects. Rotational speed Ω can be adjusted up to 3818 rpm to cover shear stresses ranging from 24 to 842 Pa. Measured hemolysis indices are shown in Fig. 1b.

Energy dissipation rate ϵ in a Couette-type shear device is given by

$$\epsilon = \tau : \nabla v = \mu(U/h) \cdot (U/h) = \mu(U/h)^2, \tag{5}$$

where τ represents the shear stress in the gap, μ is the blood viscosity (5 mPa s, as reported in Boehning et al. 2014), v represents velocity, U is the circumferential velocity of the rotor, h is the width of the gap (50 microns). The resulting sets of \bar{h} and ϵ are shown in Table 1. Based on these data, the new empirical correlation was obtained, with an R -square value of 0.91:

$$\bar{h} = \left[a \cdot (\epsilon \times 10^{-7})^2 + b \cdot \epsilon \times 10^{-7} \right] / \left[(\epsilon \times 10^{-7})^2 + c \cdot \epsilon \times 10^{-7} + d \right], \tag{6}$$

Table 1 Energy dissipation rates versus hemolysis rates for Aachen shearing device

| τ (Pa) | ϵ (W/m ³) | t (ms) | \bar{h} |
|-------------|--------------------------------|----------|-----------|
| 24 | 1.157×10^5 | 54 | 0.063 |
| | | 873 | 0.032 |
| 592 | 7.006×10^7 | 54 | 0.331 |
| | | 873 | 0.968 |
| 702 | 9.852×10^7 | 54 | 0.496 |
| | | 873 | 1.837 |
| 842 | 1.417×10^8 | 54 | 3.172 |
| | | 873 | 4.089 |

where the constants were determined as: $a = -1$, $b = 15.88$, $c = -36.44$, $d = 326.7$. Then the energy-dissipation-based power-law formulation for hemolysis is given by

$$HI(\%) = \bar{h} \cdot t. \tag{7}$$

This new formulation is referred to as ‘‘EDB model.’’ For turbulent flows, ϵ is the sum of viscous dissipation rate ϵ_{vis} and viscous dissipation rate ϵ_{turb} . The overall dissipation due to viscous and turbulent effects, E_{vis} and E_{turb} , can be obtained by volume integral of ϵ_{vis} and ϵ_{turb} :

$$E_{vis} = \int_V \epsilon_{vis}, \quad E_{turb} = \int_V \epsilon_{turb} \tag{8}$$

where V represents a specific domain. E_{vis} and E_{turb} have a unit of W .

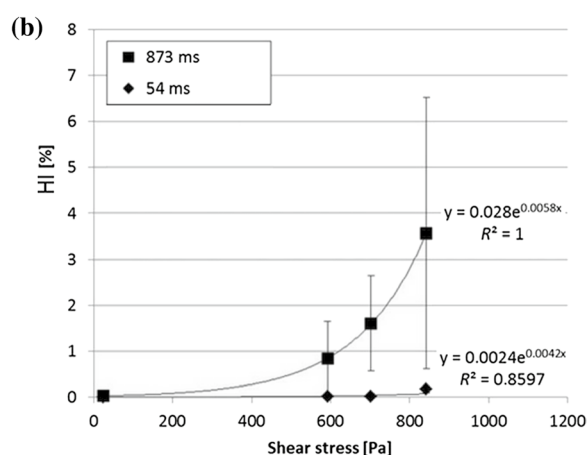
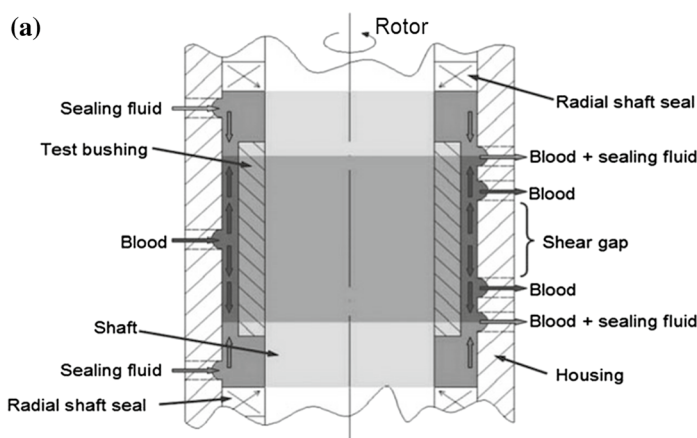


Fig. 1 a Cross section of the Aachen shearing device; (b) HI (%) for varying shear stresses at low (54 ms) and high (873 ms) exposure times (Boehning et al. 2014)

2.1 Test cases and computational setup

Three benchmark cases previously employed for the study of hemolysis in transitional and turbulent flows were investigated. The computational setup of the CFD calculations has been verified by Wu et al. (2019), in which similar conditions of the same three cases were tested. The CFD results were validated against experimental results, and a mesh sensitivity analysis with regard to pressure difference and hemolysis was conducted. Therefore, the same computational setup and grids as in Wu et al. (2019) were used. All simulations were conducted using ANSYS Fluent (Ansys, Inc., Canonsburg, PA, USA), and Reynolds stress τ_r was

modeled using RNG k- ϵ model for all cases. Blood was regarded as a Newtonian fluid.

2.1.1 Capillary tube

The first benchmark considered a capillary tube, used by Kameneva et al. (2004), which was fitted with conical connectors of length 0.008 m on both ends to let the flow fully develop at the entrance and exit. The diameter of the capillary tube was 1 mm with a length of 70 mm (cf. Figure 2). Washed bovine red cells in PBS at a 24% hematocrit circulated through the capillary in a closed loop for 90 min. RBC suspensions in saline with viscosity of 2.0 mPa s were used

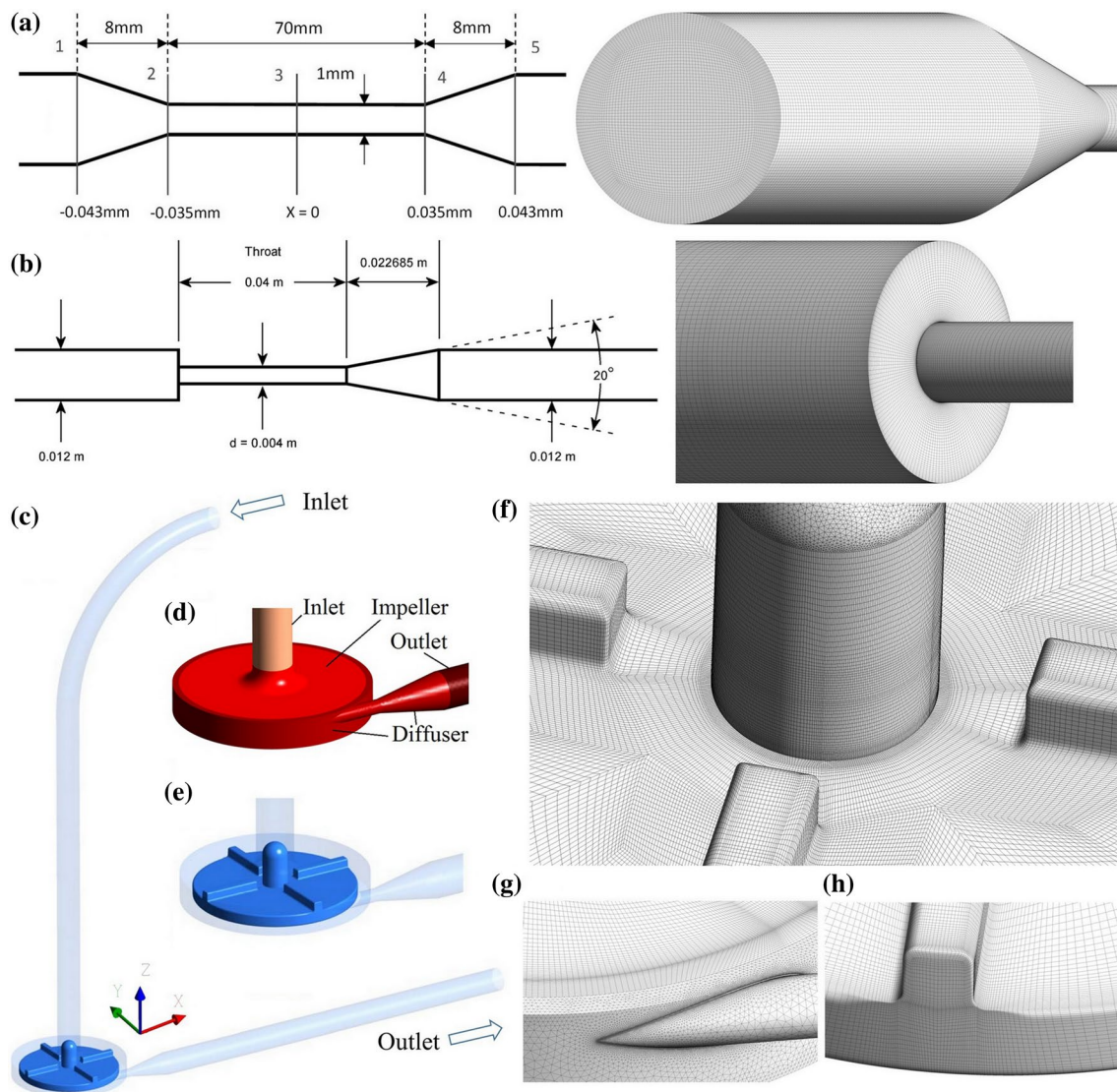


Fig. 2 **a** Schematic and mesh of the capillary tube (entrance); **b** schematic of the FDA nozzle model (conical diffuser) and its mesh; **c–e** schematic of the FDA blood pump. Details of the surface mesh at

impeller region (**g**), the interface of pump casing and discharge (**h**) and the blade trailing edge (**i**)

to study transitional and turbulent flows over flow rates ranging from 0.21 to 0.48 L/min.

Table 2 lists the cases which were investigated in this study, covering Reynolds number from 300 to 5100. The computational mesh was block structured (cf. Fig. 1b) with nearly 4 million elements. The Reynolds number at the inlet, Re_d , was well below 2000 for all the cases, therefore parabolic velocity profiles were imposed at the inlet. Four laminar conditions were also considered, with RNG $k - \epsilon$ turbulence model applied. Generally speaking, it is inappropriate to apply turbulence modes to laminar flow. Nonetheless, since the flow regimes in blood-circulating devices are mostly low-Reynolds-number and transitional flows (Fraser et al. 2011), turbulence models are often applied throughout the whole computational domain, including laminar and transitional flow regions. It is worthwhile to evaluate the accuracy of hemolysis predictions for these flow regimes when turbulence model is applied. Blood viscosity was taken as 6.3 mPa s for laminar flow conditions, and 2 mPa s for turbulent flow conditions, following Kameneva et al. (2004).

2.1.2 The FDA nozzle model

The second device was the benchmark nozzle model of FDA, which was designed to assess the quality of CFD and hemolysis estimation in device modeling. The nozzle model can be alternated to change the flow direction, referred to as “sudden expansion model” and “conical diffuser model,” respectively. Hemolysis (Herbertson et al. 2015) and PIV measurements (Hariharan et al. 2011) of velocity and pressure were acquired for both models. Figure 2 shows the schematic of the “conical diffuser model,” which features sudden contraction and a conical diffuser. Hemolysis was measured using bovine blood. Hematocrit was around 36%. The “conical diffuser model” generated significantly more hemolysis than the “sudden expansion model,” and is investigated in this study.

Table 2 Overview of conditions studied for capillary tube

| Flow rate (L/min) | μ (mPa s) | Re_d | Flow regime | Measured HI(%) |
|-------------------|---------------|--------|-------------|-----------------------|
| 0.09 | 6.3 | 300 | Laminar | 7.29×10^{-4} |
| 0.16 | 6.3 | 550 | Laminar | 8.07×10^{-4} |
| 0.23 | 6.3 | 800 | Laminar | 1.41×10^{-3} |
| 0.29 | 6.3 | 1000 | Laminar | 2.56×10^{-3} |
| 0.21 | 2.0 | 2230 | Turbulent | 8.34×10^{-4} |
| 0.33 | 2.0 | 3500 | Turbulent | 9.39×10^{-4} |
| 0.42 | 2.0 | 4500 | Turbulent | 3.79×10^{-3} |
| 0.48 | 2.0 | 5100 | Turbulent | 8.50×10^{-3} |

Re_d , the Reynolds number based on the average velocity and the diameter of the tube throat

For the FDA nozzle model, two conditions of the “conical diffuser model” were considered, and are listed in Table 3. The structured mesh contains a total of around 3.4 million cells (cf. Fig. 2b).

2.1.3 The FDA blood pump

The third test case is the FDA blood pump (cf. Fig. 2c), which was designed to access the accuracy and credibility of CFD in the prediction of flow field and hemolysis for blood pumps. The FDA blood pump has simple geometrical features, with an acrylic rotor (5.2 cm in diameter) having four filleted blades (3 mm tall and 3 mm wide) orthogonally positioned on a 4-mm-thick rotor base, and attached to a stainless steel shaft (3.2 mm in diameter) (Malinauskas et al. 2017). Both PIV and hemolysis tests were carried out for six operating conditions, with flow rates ranging from 2 to 7 L/min and rotational speeds ranging from 2500 to 3500 rpm. Porcine blood was used in hemolysis measurements with 16 replicates for each operating condition. The hematocrit was adjusted to 36%, and viscosity was 3.4 mPa s. Each hemolysis test was run for a total of 120 min, and samples were drawn every 40 min.

For this study, three operating conditions were considered for the FDA blood pump (Table 4). For the CFD setup, the pump was cut by a cylindrical surface, which acts as an interface between the rotating mesh of the impeller region and the stationary mesh of the rest. A hybrid mesh with 7 million elements was employed (cf. Fig. 2f–h). The grid in the impeller region was structured and hexahedral, while the rest of the domain was meshed using tetrahedral elements with prism layers. The tip and hub clearances were meshed using 20 layers. The “sliding mesh” approach was used to couple the rotational and stationary frames. The measured velocity profiles were applied at the inlet. Blood viscosity

Table 3 Overview of conditions studied for FDA benchmark nozzle model

| Flow rate (L/min) | Re_d | μ (mPa s) | Measured HI(%) |
|-------------------|--------|---------------|------------------------|
| 5 | 6650 | 4.21 | 2.92×10^{-5} |
| 6 | 8020 | 4.21 | 1.239×10^{-4} |

Re_d , the Reynolds number based on the average velocity and dimensions of the throat

Table 4 Overview of conditions studied for the FDA blood pump

| Flow rate (L/min) | Pump speed(rpm) | Measured HI(%) |
|-------------------|-----------------|-----------------------|
| 6 | 2500 | 7.93×10^{-5} |
| 6 | 3500 | 7.82×10^{-5} |
| 7 | 3500 | 2.44×10^{-4} |

Table 5 Constants of three commonly used power-law models

| Model | c | α | β |
|-------|------------------------|----------|---------|
| GW | 3.620×10^{-5} | 2.4160 | 0.7850 |
| HO | 1.800×10^{-4} | 1.9910 | 0.7650 |
| TZ | 1.228×10^{-5} | 1.9918 | 0.6606 |

GW, model of Giersiepen et al. (1990). TZ, model of Zhang et al. (2011). HO, model of Heuser and Opitz (1980), constants by Song et al. (2003)

was set to 3.4 mPa s. Each rotor rotation was resolved using 240 time steps. Maximum 25 sub-iterations were used for each physical time step, and convergence criteria were set that the residuals of the all equations drop 3 magnitudes, generally from 10^{-3} to 10^{-6} .

2.2 Hemolysis predictions

Hemolysis was calculated using an Eulerian scalar transport approach. Here, hb' was introduced as a scalar variable equal to $hb^{1/\beta}$. Then the power-law model, given by Eq. 1, can

be reorganized into a scalar transport equation (Garon and Farinas, 2004)

$$\frac{d(hb')}{dt} + \nu\rho \cdot \nabla(hb') = C, \tag{9}$$

where C is the source term defined as either (for conventional power-law models)

$$C = \rho(Hb \cdot c \cdot \tau_{\text{eff}}^\alpha)^{1/\beta}, \tag{10}$$

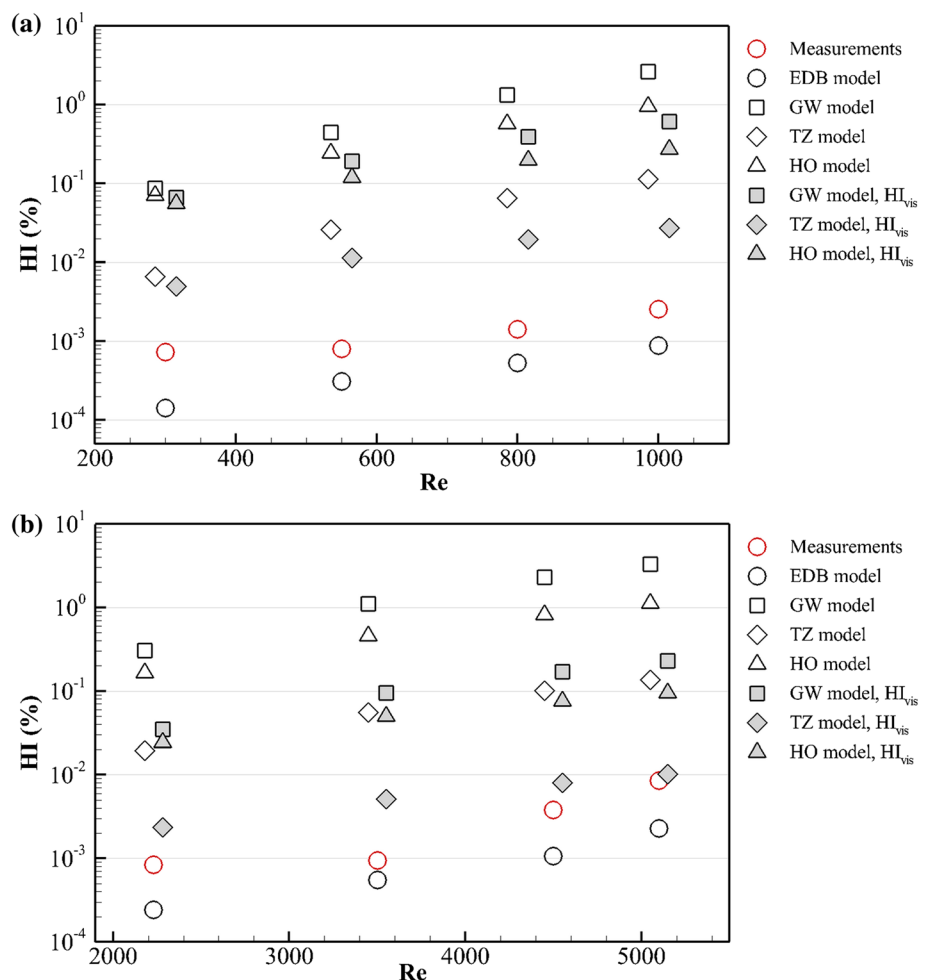
or (for EDB model)

$$C = \rho \cdot Hb \cdot 1.467 \times 10^{-2} \cdot (\epsilon \times 10^{-7})^{2.12}. \tag{11}$$

Total dissipation rate ϵ was taken as the sum of viscous and turbulent dissipation, ϵ_{vis} and ϵ_{turb} , both of which were obtained through UDF (user defined function) of ANSYS Fluent. The HI(%) was then calculated from the mass-weighted average of hb at the outlet of the device divided by Hb .

The source term C is contributed by both viscous and turbulent terms (τ_{vis} and τ_{turb} for conventional hemolysis

Fig. 3 Predicted HI(%) of the capillary tube using the EDB, GW, TZ and HO models (with either τ_{vis} or τ as effective stress), in comparison with measurements, for: **a** laminar conditions; **b** turbulent conditions



models, cf. Eq. 2; ε_{vis} and $\varepsilon_{\text{turb}}$ for the EDB model). To study the relative importance of viscous and turbulent terms to hemolysis, C_{vis} and C_{turb} were introduced to represent the effective source terms of hemolysis due to viscous and turbulent effects, respectively, while HI_{vis} and HI_{turb} were introduced to represent the individual contributions of C_{vis} and C_{turb} to hemolysis.

As aforementioned, the representation of effective stress as the sum of Reynolds stress and viscous stress (cf. Eq. 2) has been found to overestimate hemolysis; another common practice is to leave out the term of Reynolds stress and just keep the viscous stress τ_{vis} , with the corresponding hemolysis being HI_{vis} .

The EDB model, together with three conventional hemolysis models (with either τ_{vis} or τ as effective stress) listed in Table 5, was investigated. For the capillary tube, eight conditions were studied, leading to 56 cases. Hemolysis estimations were limited to the flow rates of 5 L/min and 6 L/min for the FDA benchmark nozzle, thus 14 cases were studied. As for the FDA blood pump, hemolysis calculations were carried out for all the operating conditions listed in Table 4, resulting in 21 cases.

3 Results

3.1 Capillary tube

Figure 3 shows the predicted hemolysis in the capillary tube using the GW, TZ, HO and EDB models, respectively. Overall, the results of the EDB model were in much better agreement with the measurements. The trend of the hemolysis predicted using the EDB model was in much better agreement with the measurements. The exception was found at the $\text{Re}=300$ and 2230 , for which the measured hemolysis was almost the same as $\text{Re}=550$ and 3500 , respectively, deviating from the trend from $\text{Re}=550$ – 1000 and 3500 – 5100 . The reason was unclear, possibly due to experimental uncertainties. Conventional GW, TZ and HO models over-predicted hemolysis, for both τ_{vis} and τ as effective stress. The slopes of the three conventional power-law models were significantly lower than the measurements. It is also worth to note that the HI_{vis} was closer to the experimental results and more than one order lower than the HI for all the models.

Figure 4a shows the predicted E_{turb} along with E_{vis} . Though E_{turb} is below the E_{vis} for all the investigated Reynolds numbers, $E_{\text{turb}}/E_{\text{vis}}$ steadily rises from 0.5 to nearly 0.75, which shows increasing turbulent intensities over Reynolds number.

Figure 4b shows the HI_{turb} and HI_{vis} versus Reynolds number. For all the models, the ratio $\text{HI}_{\text{turb}}/\text{HI}_{\text{vis}}$ increases with Reynolds number. While E_{vis} and E_{turb} are comparable, HI_{turb} is approximately one order higher than HI_{vis} for the GW, TZ

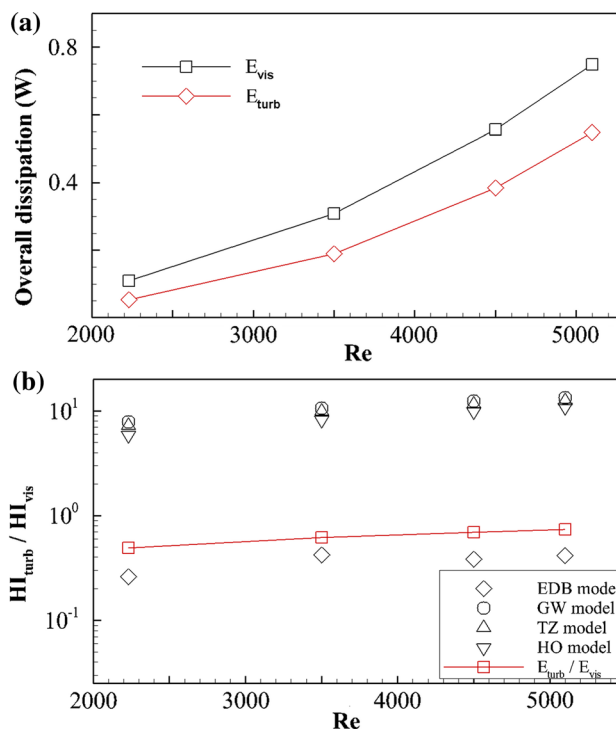


Fig. 4 **a** Overall viscous and turbulent dissipation, E_{vis} and E_{turb} , the capillary tube; **b** the ratio of contributions of viscous and turbulent terms, to hemolysis, in comparison with $E_{\text{turb}}/E_{\text{vis}}$

and HO models, even for the Reynolds number of 2230, for which laminar and transitional flow regimes are supposed to be dominant. For these models, $\text{HI}_{\text{turb}}/\text{HI}_{\text{vis}}$ is disproportional compared with $E_{\text{turb}}/E_{\text{vis}}$. For the EDB model, the ratio $\text{HI}_{\text{turb}}/\text{HI}_{\text{vis}}$ is below unity, and close to the value of $E_{\text{turb}}/E_{\text{diss}}$, indicating that viscous effects are more important than turbulence effects.

Figure 5 shows the distribution of effective sources terms C_{vis} and C_{turb} with Reynolds number of 4500 for the EDB and HO models. While the levels of C_{vis} are actually comparable for the two models, C_{turb} with HO model is disproportional compared with the level of turbulent dissipation E_{turb} , and much higher than that of EDB model, mostly occurring in central part of the diffuser, where the unsteadiness is high but turbulent dissipation is not necessarily high.

3.2 FDA nozzle model

Figure 6 shows the predicted hemolysis of the FDA nozzle model. While all the models overestimated the hemolysis, the results computed by the EDB model are closest to the experimental results. For the conventional models, though the values of HI_{vis} were much higher than the experimental results, they were around two orders lower than the HI.

Table 6 shows the predicted $E_{\text{turb}}/E_{\text{diss}}$ and $\text{HI}_{\text{turb}}/\text{HI}_{\text{vis}}$ values for the EDB and HO models. The ratio $E_{\text{turb}}/E_{\text{diss}}$

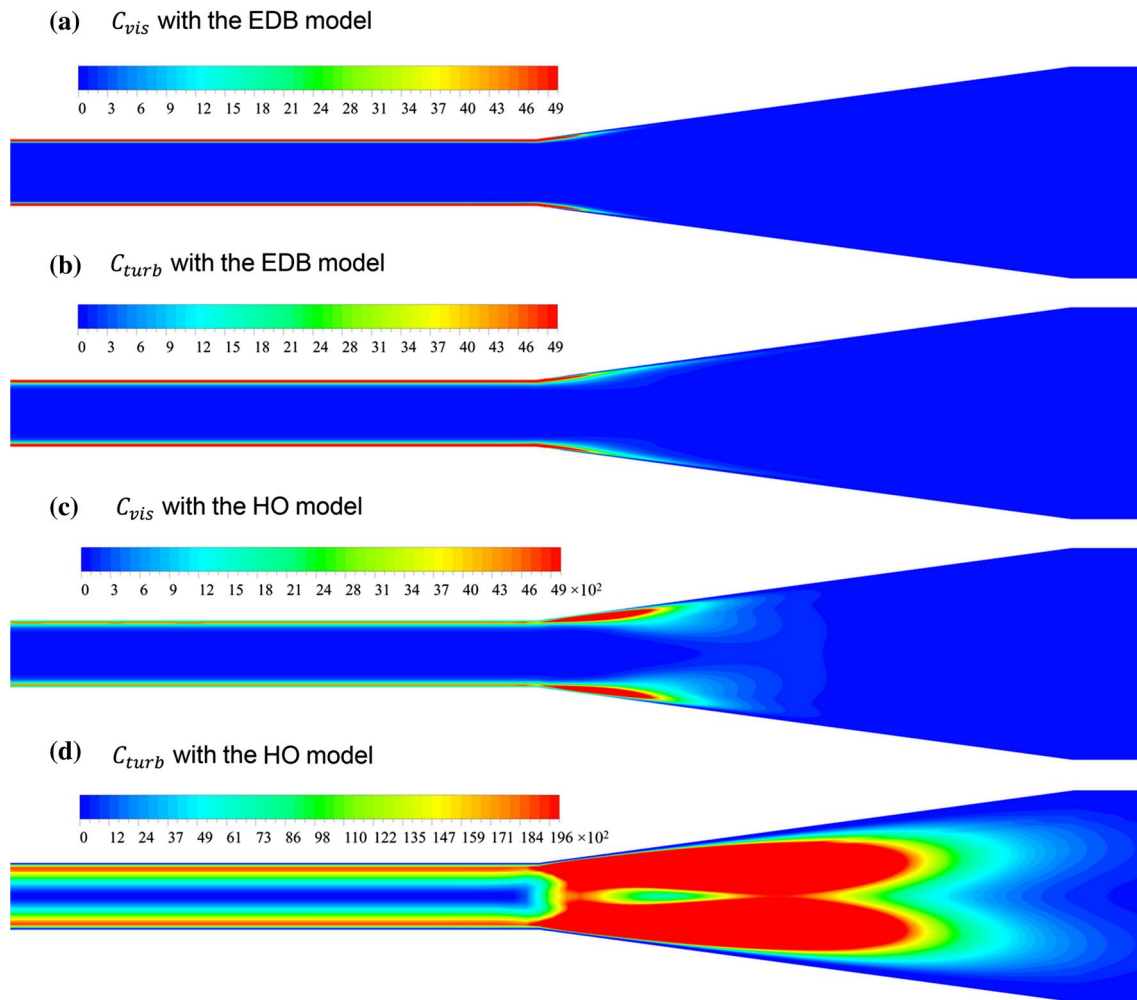


Fig. 5 Distribution of effective source terms for $Re=4500$ in Kameneva's capillary tube, **a** C_{vis} with the EDB model, **b** C_{turb} with the EDB model, **c** C_{vis} with the HO model and **d** C_{turb} with the HO model

increases from 5.41 to 6.15 as flow rate increases, indicating increasing turbulent intensity. However, concerning the ratio HI_{turb}/HI_{vis} , the contribution of turbulent and viscous effects to hemolysis for the HO model is of order 10^2 . Therefore, turbulent effects were associated with 20 times more blood damage than viscous effects. In contrast, HI_{turb}/HI_{vis} for the EDB model is at the same order as E_{turb}/E_{diss} . This can explain the over-predictions of the conventional power-law models.

3.3 FDA blood pump

The results of hemolysis prediction are shown in Fig. 7. Similar to the two previous test cases, the results from the EDB are in much better agreements with the measurements; the over-prediction of the conventional power-law model was improved. The EDB model captured the trend of hemolysis for the conditions of 6 L/min, 3500 rpm and 7 L/min,

3500 rpm, though the hemolysis at 6 L/min, 2500 rpm is under-predicted. While the HI_{vis} was more than one order lower than the HI for all the conventional models, the values of HI_{vis} at 7 L/min, 3500 rpm were even lower than 6 L/min, 2500 rpm, thus failed to capture the trend of hemolysis.

Figure 8 shows the distribution of effective sources terms C_{vis} and C_{turb} for 6 L/min, 3500 rpm. Overall, $C_{turb, HO}$ (source term of hemolysis associated with Reynolds stress for the HO model) was around 4 orders higher than $C_{vis, HO}$, while $C_{turb, EDB}$ (source term of hemolysis associated with turbulent dissipation for the EDB model) was around 1 order higher than $C_{vis, HO}$. The region "Outlet" is actually a diffuser, where flow is highly transient and Reynolds stress is very high, artificially increases the source term of hemolysis. Similar phenomena can also be observed near the blades (cf. Fig. 8b).

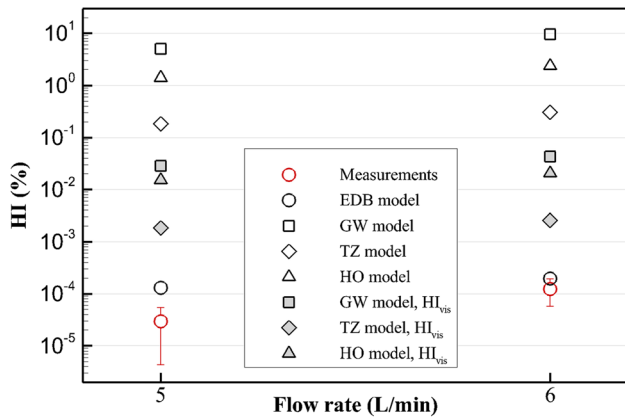


Fig. 6 Predicted hemolysis of the FDA nozzle diffuser using EDB, GW, TZ and HO models

Table 6 Predicted energy dissipation and hemolysis in the FDA nozzle model

| Condition | $E_{\text{turb}}/E_{\text{vis}}$ | $(HI_{\text{turb}}/HI_{\text{vis}})_{\text{HO}}$ | $(HI_{\text{turb}}/HI_{\text{vis}})_{\text{EDB}}$ |
|-----------|----------------------------------|--|---|
| 5 (L/min) | 5.41 | 91.4 | 1.90 |
| 6 (L/min) | 6.15 | 112.7 | 2.26 |

$(HI_{\text{turb}}/HI_{\text{vis}})_{\text{HO}}$ and $(HI_{\text{turb}}/HI_{\text{vis}})_{\text{EDB}}$, the ratio of contributions of viscous and turbulent dissipation to hemolysis, for HO model and EDB model, respectively

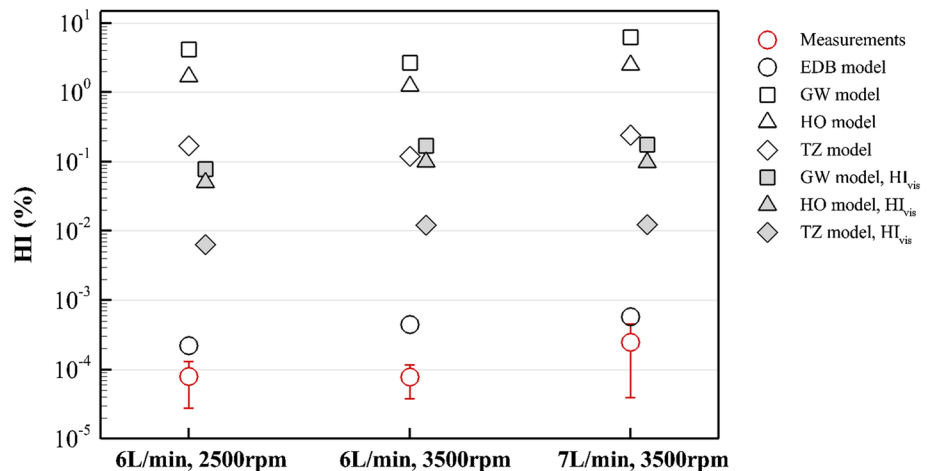
4 Discussion

Compared with conventional power-law models, the energy dissipation power-law formulation improved the prediction of hemolysis for a wide range of flow regimes. The over-prediction of hemolysis was improved, and the differences

from experimental results were within one order for most cases (cf., Figs. 3, 6 and 7). Table 7 shows the correlation coefficients of predicted hemolysis and experimental results for the capillary tube and FDA blood pump. The results of the EDB model had the best correlation with the experimental results for the tube, while their correlation with experimental results for the FDA pump sits in between those of the conventional models and HI_{vis} (results with the representation of effective stress in terms of viscous stress only). This is due to the over-prediction of hemolysis at condition 6 L/min, 3500 rpm for the EDB model. One should note an accurate representation of the flow field is the precondition for the prediction of hemolysis. As shown in Wu et al. (2019), for the off-design points of the FDA pump, the pressure head and flow field were not well captured using the RANS method. Therefore, in addition to the hemolysis model itself, the over-prediction of hemolysis might also be induced by inaccurate flow fields. Most notably, although the values of HI_{vis} are closer to the experimental results, their correlation with the experimental results is the worst, especially for the FDA blood pump.

Reynolds stresses were the main cause of over-predictions of hemolysis for conventional power-law models. Proportionally, blood damage predicted with Reynolds stresses was around 10–20 times more than viscous stress, in terms of energy dissipation. In regions such as a straight outlet tube and diffuser, where the blood damage is supposed to be low, the hemolysis predicted with conventional power-law models is comparable with that in regions such as narrow tube and regions containing highly spinning rotor. The velocity fluctuations in these regions are high (which means Reynolds stresses will be high as well), but energy dissipation is low. Therefore, using Reynolds stress to account for hemolysis leads to overestimation of hemolysis in these regions.

Fig. 7 Predicted hemolysis of the FDA blood pump in comparison with measurements, using EDB, GW, TZ and HO models



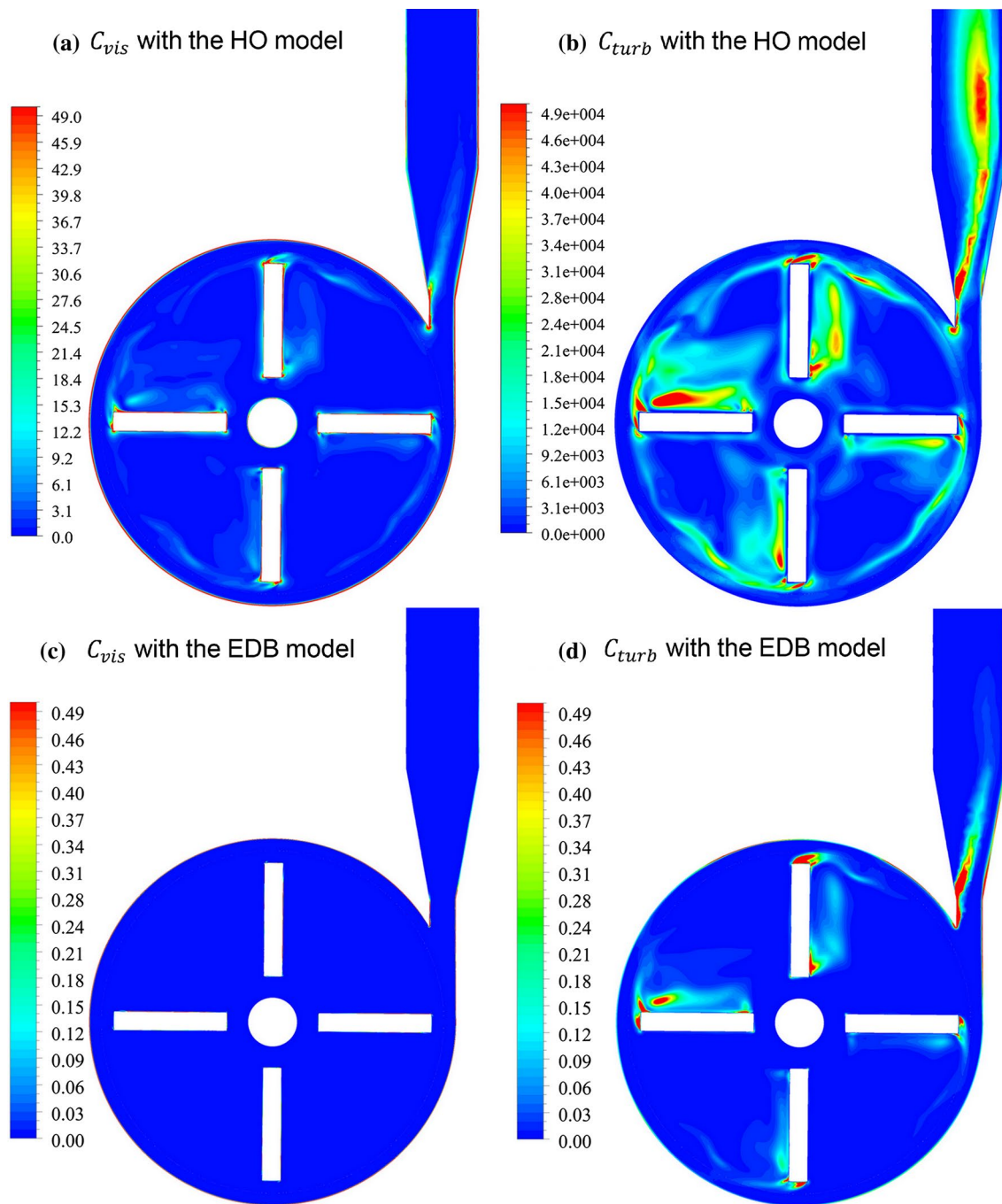


Fig. 8 Distribution of effective source terms for 6 L/min, 3500 rpm of the FDA blood pump at plane XY (cf. Fig. 2d) **a** C_{vis} with the HO model, and **b** C_{turb} with the HO model, **c** C_{vis} with the EDB model, **d** C_{turb} with the EDB model

Table 7 Correlation coefficients of predicted hemolysis and experimental results, for the capillary tube and FDA blood pump

| Case | GW | TZ | HO | GW, HI_{vis} | TZ, HI_{vis} | HO, HI_{vis} | EDB |
|------------------|--------|--------|--------|----------------|----------------|----------------|--------|
| Tube (laminar) | 0.9909 | 0.9805 | 0.9761 | 0.9648 | 0.9448 | 0.9404 | 0.9914 |
| Tube (turbulent) | 0.9460 | 0.9285 | 0.9275 | 0.9277 | 0.9066 | 0.9007 | 0.9785 |
| Pump | 0.9102 | 0.9116 | 0.9402 | 0.5492 | 0.5440 | 0.4868 | 0.7786 |

5 Limitation

In this study, an energy-dissipation-based model of hemolysis prediction was proposed. It was built with limited hemolysis data and is still a preliminary model. The coefficients were regressed from existing hemolysis data of only two exposure times. Hemolysis was assumed to vary linearly with exposure time. However, as previous studies indicated, the power of exposure time in hemolysis relationships is normally below one. Although the hemolysis data covered a broad range of stresses (24–842 Pa), the number of data points was not sufficient, especially the data in the range of (24–592 Pa) have to be included for hemolysis relationship with low stress or energy dissipation. More data will be needed to cover a broad range of stress and exposure time. Moreover, the hemolysis data which were used to build the EDB model show large standard deviations. More measurement replicates will be helpful to reduce the standard variation. The EDB model did not account for the influence of blood species. Blood from different species has been shown to have different hemolytic responses (Ding, et al. 2015). For the future investigations, the influence of blood species should be incorporated. Nonetheless, this work represents the first attempt to build an energy-dissipation model based on existing experimental hemolysis data. The energy-dissipation-based model remarkably improved the prediction of hemolysis, in terms of both absolute values and correlation coefficients. Hopefully, this work will serve as a modest spur to induce more valuable contributions.

As aforementioned, RANS turbulence prediction method was used in this study, which often fails to capture complex transitional and turbulent flows. This brings errors to the prediction of hemolysis. Therefore, the influence of prediction of flow field on the accuracy of hemolysis predictions should be explored, and more advanced turbulence modeling method should be employed in the future.

6 Conclusion

This study proposed an energy-dissipation-based formulation for estimating hemolysis based on published experimental hemolysis data. Hemolysis was related to the energy dissipation rate, which can be obtained from CFD simulations. The new formulation was tested for three benchmark cases, together with three conventional power-law models. The results showed that the EDB model improved the prediction of the hemolysis, for a broad range of flow regimes. The over-prediction was improved, and the deviations from experimental results were within one order for almost all cases. The results of the EDB model are also better correlated with experimental results in general.

This study found Reynolds stress is the main cause of over-prediction of hemolysis for conventional power-law models. Proportionally, the blood damage predicted with Reynolds stresses is around 10–20 times higher than viscous stress, in terms of energy dissipation. In certain regions where unsteadiness is high (Reynolds stresses will be high as well), while energy dissipation is low, Reynolds stress was the primary cause of hemolysis and the differences between the EDB model and conventional power-law models are even more pronounced.

This study also investigated the representation of effective stress using viscous stress only. Though the over-prediction of hemolysis was improved compared with the inclusion of Reynolds stress in the effective stress, the average correlation coefficient of predicted hemolysis and experimental results is merely 0.7192.

Acknowledgements The authors would like to acknowledge the coordinated support from Natural Science Foundation of China (Grant No. 51406127) and Natural Science Foundation of Jiangsu Province (Grant No. BK20140344).

Compliance with ethical standards

Conflict of interest The authors declare that they have no conflicts of interest.

References

- Arvand A, Hormes M, Reul H (2005) A validated computational fluid dynamics model to estimate hemolysis in a rotary blood pump. *Artif Organs* 29:531–540
- Boehning F, Mejia T, Schmitz-Rode T, Steinseifer U (2014) Hemolysis in a laminar flow-through Couette shearing device: an experimental study. *Artif Organs* 38:761–765
- Cao SJ, Meyers J (2012) On the construction and use of linear low-dimensional ventilation models. *Indoor Air* 22:427–441
- Cao SJ, Cen D, Zhang W, Feng Z (2017) Study on the impacts of human walking on indoor particles dispersion using momentum theory method. *Build Environ* 126:195–206
- Chen Y, Sharp MK (2011) A strain-based flow-induced hemolysis prediction model calibrated by in vitro erythrocyte deformation measurements. *Artif Organs* 35:145–156
- Ding J, Niu S, Chen Z, Zhang T, Griffith BP, Wu ZJ (2015) Shear-induced hemolysis: species differences. *Artif Organs* 39:795–802
- Ezzeldin HM, de Tullio MD, Vanella M, Solares SD, Balaras E (2015) A strain-based model for mechanical hemolysis based on a coarse-grained red blood cell model. *Annals Biomed Eng* 43:1398–1409
- Faghih MM, Sharp MK (2018) Characterization of erythrocyte membrane tension for hemolysis prediction in complex flows. *Biomech Model Mechanobiol* 17:827–842
- Fraser KH, Taskin ME, Griffith BP (2011) The use of computational fluid dynamics in the development of ventricular assist devices. *Med Eng Phys* 33:263–280
- Garon A, Farinas M (2004) Fast Three-dimensional numerical hemolysis approximation. *Artif Organs* 28:1016–1025
- Ge L, Dasi L, Sotiropoulos F, Yoganathan AJ (2008) Characterization of hemodynamic forces induced by mechanical heart valves: Reynolds vs. viscous stresses. *Annals Biomed Eng* 36:276–297

- Giersiepen M, Wurzingler LJ, Opitz R, Reul H (1990) Estimation of shear stress-related blood damage in heart valve prostheses-in vitro comparison of 25 aortic valves. *Int J Artif Organs* 13:300–306
- Grigioni M, Caprari P, Tarzia A, D'Avenio G (2005) Prosthetic heart valves' mechanical loading of red blood cells in patients with hereditary membrane defects. *J Biomech* 38:1557–1565
- Hariharan P, Giarra M, Reddy V, Day SW, Manning KB, Deutsch S, Stewart SF, Myers MR, Berman MR, Burgreen GW, Paterson EG (2011) Multilaboratory particle image velocimetry analysis of the FDA benchmark nozzle model to support validation of computational fluid dynamics simulations. *J Biomech Eng* 133:041002
- Herbertson LH, Olia SE, Daly A, Noatch CP (2015) Multilaboratory study of flow-induced nozzle model. *Artif Organs* 39:237–259
- Heuser G, Opitz RA (1980) Couette viscometer for short-time shearing of blood. *Biorheology* 17:17–24
- Hund SJ, Antaki JF, Massoudi M (2010) On the representation of turbulent stresses for computing blood damage. *Int J Eng Sci* 48:1325
- Jones SA (1995) A relationship between Reynolds stresses and viscous dissipation: implications to red cell damage. *Annals Biomed Eng* 23:21–28
- Kameneva MV, Burgreen GW, Kono K, Repko B, Antaki JF, Umezumi M (2004) Effects of turbulent stresses upon mechanical hemolysis: experimental and computational analysis. *ASAIO J* 50:418–423
- Malinauskas RA, Hariharan P, Day SW, Herbertson LH, Buesen M, Steinseifer U, Aycok KI, Good BC, Deutsch S, Manning KB, Craven BA (2017) FDA benchmark medical device flow models for CFD validation. *ASAIO J* 63:150–160
- Morshed KN, Bark D Jr, Forleo M, Dasi LP (2014) Theory to predict shear stress on cells in turbulent blood flow. *PLoS ONE* 9:e105357
- Park SJ, Tector A, Piccioni W, Raines E, Gelijns A, Moskowitz A, Rose E, Holman W, Furukawa S, Frazier OH, Dembitsky W (2005) Left ventricular assist devices as destination therapy: a new look at survival. *J Thorac Cardiovasc Surg* 129:9–17
- Pope SB (2000) *Turbulent flows*. Cambridge University Press, Cambridge
- Quinlan NJ (2014) Mechanical loading of blood cells in turbulent flow. In: Doyle B, Miller K, Wittek A, Nielsen MFP (eds) *Computational biomechanics for medicine: fundamental science and patient-specific applications*. Springer, New York, pp 1–13
- Quinlan NJ, Dooley P (2007) Models of flow-induced loading on blood cells in laminar and turbulent flow, with application to cardiovascular device flow. *Annals Biomed Eng* 35:1347–1356
- Rose EA, Gelijns AC, Moskowitz A, Heitjan DF, Stevenson LW (2001) Long-term use of a left ventricular assist device for end-stage heart failure. *N Engl J Med* 345:1435–1443
- Segalova PA, Rao KTV, Zarins CK, Taylor CA (2012) Computational modeling of shear-based hemolysis associated with renal obstruction. *J Biomech Eng* 134:021003
- Sohrabi S, Liu Y (2017) A cellular model of shear-induced hemolysis. *Artif Organs* 35:1180–1186
- Song X, Throckmorton AL, Wood HG, Antaki JF, Olsen DB (2003) Computational fluid dynamics prediction of blood damage in a centrifugal pump. *Artif Organs* 27:938–941
- Vitale F, Nam J, Turchetti L, Behr M, Raphael R, Annesini MC, Pasquali M (2014) A multiscale, biophysical model of flow-induced red blood cell damage. *AIChE J* 60:1509–1516
- Wu P, Meyers J (2011) Globally conservative high-order filters for large-eddy simulation and computational aero-acoustics. *Comput Fluids* 48:150–162
- Wu P, Meyers J (2013) A constraint for the subgrid-scale stresses in the logarithmic region of high Reynolds number turbulent boundary layers: a solution to the log-layer mismatch problem. *Phys Fluids* 25:349–374
- Wu J, Paden BE, Borovetz HS, Antaki JF (2009) Computational fluid dynamics analysis of blade tip clearances on hemodynamic performance and blood damage in a centrifugal ventricular assist device. *Artif Organs* 34:402–411
- Wu P, Gross-Hardt S, Boehning F, Hsu PL (2018a) On the accuracy of hemolysis models in Couette-type blood shearing devices. *Artif Organs* 42:E290–E303
- Wu P, Feng Z, Cao SJ (2018b) Fast and accurate prediction of airflow and drag force for duct ventilation using wall-modeled large-eddy simulation. *Build Environ* 141:226–235
- Wu P, Gao Q, Hsu PL (2019) On the representation of effective stress for computing hemolysis. *Biomech Model Mechanobiol* 18(3):665–679
- Zhang T, Taskin ME, Fang HB, Pampori A, Jarvik R, Griffith BP, Wu ZJ (2011) Study of flow-induced hemolysis using novel Couette-type blood shearing devices. *Artif Organs* 35:1180–1186

Publisher's Note Springer Nature remains neutral with regard to jurisdictional claims in published maps and institutional affiliations.